



# Synthesis, structures and spectroscopic properties of new 1,2-bis[2-(4-methyl-7-acetylamino-1,8-naphthyridine)]ethylene ligand and its binuclear copper(I) complexes

Li Zhan-Xian<sup>a</sup>, Li Cong<sup>b</sup>, Mu Wei-Hua<sup>b</sup>, Xiong Shao-Xiang<sup>c</sup>, Fu Wen-Fu<sup>a,b,\*</sup>

<sup>a</sup>Key Laboratory of Photochemical Conversion and Optoelectronic Materials, HKU-CAS Joint Laboratory on New Materials, Technical Institute of Physics and Chemistry, Chinese Academy of Sciences, Peking 100190, PR China

<sup>b</sup>College of Chemistry and Chemical Engineering, Yunnan Normal University, Kunming 650092, PR China

<sup>c</sup>Beijing Mass Spectrometry Center, Center for Molecular Science, Institute of Chemistry, Chinese Academy of Sciences, Beijing 100080, PR China

## ARTICLE INFO

### Article history:

Received 27 January 2011

Received in revised form 30 August 2011

Accepted 2 September 2011

Available online 22 September 2011

### Keywords:

1,8-Naphthyridine derivatives

Vinyl

Binuclear copper(I)

Crystal structures

Spectroscopic properties

## ABSTRACT

The synthesis, characterization, spectroscopic properties of a new ligand 1,2-bis[2-(4-methyl-7-acetylamino-1,8-naphthyridine)]ethylene (**L**) and its two binuclear Cu(I) complexes containing triphenylphosphine (PPh<sub>3</sub>) or bis(diphenylphosphino)methane (dppm), [Cu<sub>2</sub>(L)(PPh<sub>3</sub>)<sub>4</sub>](BF<sub>4</sub>)<sub>2</sub>·2CH<sub>2</sub>Cl<sub>2</sub> (**1**·2CH<sub>2</sub>Cl<sub>2</sub>) and [Cu<sub>2</sub>(L)(dppm)<sub>2</sub>](BF<sub>4</sub>)<sub>2</sub>·4H<sub>2</sub>O (**2**·4H<sub>2</sub>O) are reported. The structural investigation of these compounds based on X-ray crystal analysis shows that the copper(I) centers adopt different coordination geometries, O(N)CuP<sub>2</sub><sup>+</sup> and NCuP<sub>2</sub><sup>+</sup> for complexes **1** and **2**, respectively. Upon irradiation of a degassed organic solution of **L** at 365 nm, photoinduced isomerization reaction and an intramolecular proton transfer of ligand **L** were detailed studied by absorption spectral changes. A spectroscopic investigation involving time-dependent density functional theory calculations allows assignment of the excited states that relate to emission and transient absorption spectra. The observed lower-energy absorption bands appearing in the region of 413 and 418 nm for **1** and **2** in dichloromethane are assigned to ligand-to-ligand charge transfer (LLCT, phosphine → napy) transition in nature. Compared with well-structured solid-state emission originating from ππ\* transition of ligand **L**, complexes **1** and **2** exhibit intense room-temperature solid-state emissions with λ<sub>max</sub> at 586 and 620 nm, respectively. The energy and the shape of the emission bands are clearly different from that of the ligand, indicating the emissions come from different excited states.

© 2011 Elsevier B.V. All rights reserved.

## 1. Introduction

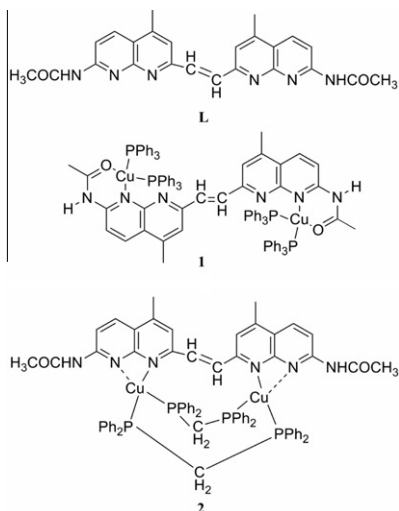
The availability of 1,8-naphthyridine and its alkyl derivatives in biological systems have been of considerable interest because of their ability to form adducts containing multiple hydrogen bonds with the nitrogenous bases of DNA [1–7]. Studies of ligand functionalized with 1,8-naphthyridine have focused on examining the behavior of this ring system [8–10], and intriguing coordination modes and bonding properties of such compounds when they are used as monodentate, bidentate and multidentate ligands [11–19]. Recently, research has been extended to the chemistry of the naphthyridine-based metal complexes [20–28], especially the luminescent multinuclear Zn(II) complexes which have potential application in materials science [29–32]. We have been involved in the study of the photochemical and photophysical properties of Cu(I) and Zn(II) complexes containing flexible 1,8-naphthyridine

derivatives [33–35]. In general, the copper(I) center in the class of complexes is three- or four-coordinated with a distorted trigonal or tetrahedral configuration. 1,8-Naphthyridine-based ligands usually exhibit chelating and bridging coordination modes, which can be ascribed to the limitation of their rigid frameworks. The investigation of the photophysical properties of luminescent naphthyridine derivatives and their copper(I) complexes demonstrated that their emissive ππ\* and metal-to-ligand charge-transfer (MLCT) excited states can be tuned by changing the environmental conditions [36]. However, the study of the photochemical and photophysical properties of copper(I) complexes with 1,8-naphthyridine-based ligands using transient absorption and time-dependent density functional theory (TD-DFT) calculations on copper(I) complexes is still inadequate.

Herein, we report the synthesis and characterization of 1,2-bis[2-(4-methyl-7-acetylamino-1,8-naphthyridine)]ethylene (**L**) and its complexes [Cu<sub>2</sub>(L)(PPh<sub>3</sub>)<sub>4</sub>](BF<sub>4</sub>)<sub>2</sub>·2CH<sub>2</sub>Cl<sub>2</sub> (**1**·2CH<sub>2</sub>Cl<sub>2</sub>) and [Cu<sub>2</sub>(L)(dppm)<sub>2</sub>](BF<sub>4</sub>)<sub>2</sub>·4H<sub>2</sub>O (**2**·4H<sub>2</sub>O) (Scheme 1), as well as their photophysical properties. Results from spectroscopic investigations involving transient absorption and TD-DFT calculations have

\* Corresponding author at: College of Chemistry and Chemical Engineering, Yunnan Normal University, Kunming 650092, PR China.

E-mail address: [fuwf@mail.ipc.ac.cn](mailto:fuwf@mail.ipc.ac.cn) (W.-F. Fu).



**Scheme 1.** The chemical structures of ligand **L** and complexes **1** and **2**.

important consequences for the photophysical behavior of 1,8-naphthyridine-based copper(I) complexes.

## 2. Experimental

### 2.1. General comments

All reactions were performed under a nitrogen atmosphere. Reagent grade solvents were dried by the standard procedures and freshly distilled prior to use.  $^1\text{H}$  NMR spectra were recorded on a Bruker 400 spectrometer at 298 K with chemical shifts ( $\delta$ , ppm) relative to tetramethylsilane ( $\text{Me}_4\text{Si}$ ) for  $^1\text{H}$ . Elemental analysis was carried out on a Carlo Erba 1106 element analytical instrument. The UV–Vis spectra were taken on a HITACHI U-3010 spectrophotometer, and the corrected emission spectra of solution and solid were obtained on a HITACHI F-4500 fluorescence spectrophotometer adapted to a right-angle configuration at room temperature. Emission lifetimes of solid or solution samples were measured with Single Photon Count Technology on a FL920 Spectrometer (Edinburgh). Transient absorption spectra were recorded on a Laser Flash Photolysis Spectrometer 920 (Edinburgh) after excitation of the sample in degassed methanol or acetone with 8 ns laser pulse at 355 nm. The optical difference spectrum was generated point by point by monitoring at individual wavelengths.

### 2.2. 2,4-Dimethyl-7-amino-1,8-naphthyridine [37]

2,6-Diamino-pyridine (10.9 g, 0.1 mol) and acetyl acetone (10.0 g, 0.1 mol) were mixed in 50 mL acetic acid, and 1.2 mL 96% sulfuric acid was added. The mixture was refluxed with stirring for 24 h under a nitrogen atmosphere. The resulting solution was then cooled to room temperature, after which 150 mL sodium hydroxide (6.67 M) solution was added slowly in an ice bath. The precipitate was isolated by filtration, and washed with cool water ( $3 \times 5$  mL) and dried in vacuum. The product was recrystallized from ethanol by slow evaporation. Yield: 5.2 g (30%); m.p.: 220–221 °C;  $^1\text{H}$  NMR (400 MHz,  $\text{CDCl}_3$ )  $\delta$  (ppm): 2.52 (s, 3H,  $\text{CH}_3$ ), 2.57 (s, 3H,  $\text{CH}_3$ ), 6.67 (d,  $J=9.7$  Hz, 1H, Naph-H), 6.89 (s, 1H, Naph-H), 7.90 (d,  $J=9.7$  Hz, 1H, Naph-H); MS (EI):  $m/z$  (%): 173 ( $M^+$ ). Anal. Calc. for  $\text{C}_{10}\text{H}_{11}\text{N}_3$  (173.21): C, 69.34; H, 6.40; N, 24.26. Found: C, 69.17; H, 6.38; N, 24.41%.

### 2.3. 2,4-Dimethyl-7-acetylmino-1,8-naphthyridine

About 4 g (0.0231 mol) 2,4-dimethyl-7-amino-1,8-naphthyridine was added to 15 mL diacetyl oxide. The mixture was refluxed with stirring for 1 h under a nitrogen atmosphere and concentrated in vacuum to give the crude product. The product was recrystallized from ethanol. Yield: 3.97 g (80%).

### 2.4. 7-Acetylmino-4-methyl-1,8-naphthyridine-2-aldehyde

About 4 g (0.0186 mol) 2,4-dimethyl-7-acetylmino-1,8-naphthyridine and 3.092 g (0.0278 mol) selenium dioxide were added in 200 mL 1,4-dioxane, the mixture was refluxed with stirring for 4 h under a nitrogen atmosphere [38,39]. The resulting mixture was filtered while hot, and the filtrate was concentrated down to 10 mL in vacuum. Dichloromethane (200 mL) was added and the resulting solution was extracted with water ( $2 \times 80$  mL). The organic fraction was dried over  $\text{Na}_2\text{SO}_4$  and the solvent was evaporated to give the crude product. The product was purified by column chromatography over silica gel column using dichloromethane/ethanol (30/1, v/v) as the eluent. Yield: 1.49 g (35%).  $^1\text{H}$  NMR ( $\text{CDCl}_3$ , 400 MHz)  $\delta$  (ppm): 2.34–2.37 (s, 3H,  $\text{COCH}_3$ ), 2.83–2.87 (s, 3H,  $\text{CH}_3$ ), 7.87 (s, 1H, NH), 8.38–8.40 (m, 1H, Napy), 8.65–8.67 (d, 2H, Napy), 10.19 (s, 1H, CHO). ESI MS  $m/z$  (%): 229 ( $M^+$ ) (100%), 214, 186, 173, 160, 144, 131. Anal. Calc. for  $\text{C}_{12}\text{H}_{11}\text{N}_3\text{O}_2$  (229.23): C, 62.87; H, 4.84; N, 18.33. Found: C, 62.85; H 4.86; N, 18.31%.

### 2.5. 1,2-Bis[2-(4-methyl-7-acetylmino-1,8-naphthyridine)]ethylene (L)

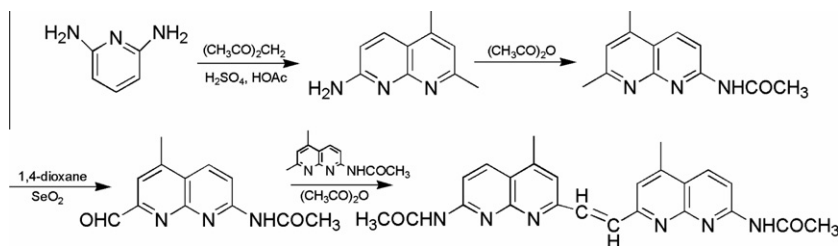
About 1.343 g (6.2 mmol) 2,4-dimethyl-7-acetylmino-1,8-naphthyridine and 1.430 g (6.2 mmol) 7-acetylmino-4-methyl-1,8-naphthyridine-2-aldehyde were mixed in 15 mL diacetyl oxide. The mixture was refluxed and stirred for 24 h under a nitrogen atmosphere. The resulting solution was added in 100 mL ice water while hot, and then filtered after stirring for 1 h. The crude product was recrystallized from ethanol, and then separated by column chromatography over silica gel column using chloroform/ethanol (20/1, v/v) as eluent. Yield: 0.4 g (15%).  $^1\text{H}$  NMR (400 MHz  $\text{CDCl}_3$ )  $\delta$  (ppm): 2.74–2.76 (s, 6H,  $\text{COCH}_3$ ), 2.97 (s, 6H,  $\text{CH}_3$ ), 8.41 (s, 2H, NH), 8.52–8.54 (d, 2H,  $\text{CH}=\text{CH}$ ), 8.69 (d, 2H, Napy), 8.76 (d, 2H, Napy), 8.93–8.95 (d, 2H, Napy). ESI MS  $m/z$  (%): 426 ( $M^+$ ) (100%), 341, 173, 146. Anal. Calc. for  $\text{C}_{24}\text{H}_{22}\text{N}_6\text{O}_2$  (426.47): C, 67.59; H, 5.20; N, 19.71. Found: C, 67.57; H, 5.21; N, 19.30%.

### 2.6. $\text{Cu}_2(\text{L})(\text{PPh}_3)_4(\text{BF}_4)_2 \cdot 2\text{CH}_2\text{Cl}_2$ (**1**· $2\text{CH}_2\text{Cl}_2$ )

Ligand **L** 0.085 g (0.2 mmol),  $\text{Cu}(\text{CH}_3\text{CN})_4\text{BF}_4$  0.1258 g (0.4 mmol) and  $\text{PPh}_3$  0.2096 g (0.8 mmol) were dissolved in the mixed solvents of dichloromethane and methanol. After stirring for 2 h at room temperature, the mixture was evaporated to dryness in vacuum leaving an orange solid. Recrystallization of the crude product from a dichloromethane/diethyl ether solution afforded an orange crystal. Yield: 0.2336 g (60%). The crystalline solid was characterized by  $^1\text{H}$  NMR and X-ray crystallography.  $^1\text{H}$  NMR (400 MHz  $\text{CDCl}_3$ )  $\delta$  (ppm): 2.54 (s, 6H,  $\text{COCH}_3$ ), 2.92 (s, 6H,  $\text{CH}_3$ ), 7.31–7.41 (60H, Ph), 7.51–7.53 (d, 2H,  $\text{CH}=\text{CH}$ ), 7.55–7.53 (d, 2H, Napy), 7.65–7.67 (d, 2H, Napy), 7.67–7.70 (d, 2H, Napy). ESI MS:  $m/z$  (%): 1690 [powders,  $M-\text{BF}_4^-$ ] $^+$ . Anal. Calc. for  $\text{C}_{98}\text{H}_{86}\text{B}_2\text{Cl}_4\text{Cu}_2\text{F}_8\text{N}_6\text{O}_2\text{P}_4$  (crystals, 1946.18): C, 60.48; H, 4.45; N, 4.32. Found: C, 60.25; H, 4.32; N, 4.57%.

### 2.7. $\text{Cu}_2(\text{L})(\text{dppm})_2(\text{BF}_4)_2 \cdot 4\text{H}_2\text{O}$ (**2**· $4\text{H}_2\text{O}$ )

A mixture of ligand **L** 0.0852 g (0.2 mmol),  $\text{Cu}(\text{CH}_3\text{CN})_4\text{BF}_4$  0.1258 g (0.4 mmol) and dppm 0.1538 g (0.4 mmol) in dichloro-

Scheme 2. Synthetic route of **L**.**Table 1**  
Summary of X-ray crystallographic data for **1** and **2**.

Complex	<b>1</b>	<b>2</b>
Formula	C <sub>96</sub> H <sub>82</sub> B <sub>2</sub> Cu <sub>2</sub> F <sub>8</sub> N <sub>6</sub> O <sub>2</sub> P <sub>4</sub> ·2CH <sub>2</sub> Cl <sub>2</sub>	C <sub>74</sub> H <sub>66</sub> B <sub>2</sub> Cu <sub>2</sub> F <sub>8</sub> N <sub>6</sub> P <sub>4</sub> O <sub>2</sub> ·4H <sub>2</sub> O
Formula weight	1946.11	1568.03
T (K)	293(2)	293(2)
Crystal system	triclinic	monoclinic
Space group	<i>P</i> $\bar{1}$	<i>P</i> 2(1)
Crystal size (mm)	0.22 × 0.20 × 0.18	0.25 × 0.10 × 0.06
<i>a</i> (Å)	12.106(2)	14.1417(3)
<i>b</i> (Å)	12.984(2)	17.0832(4)
<i>c</i> (Å)	16.320(3)	16.6051(6)
$\alpha$ (°)	81.514(3)	90.00
$\beta$ (°)	72.605(3)	106.3803(8)
$\gamma$ (°)	74.343(3)	90.00
<i>V</i> (Å <sup>3</sup> )	2351.0(7)	3848.7(2)
<i>Z</i>	1	2
<i>D</i> <sub>calc</sub> (g cm <sup>-3</sup> )	1.375	1.351
<i>F</i> (000)	1000	1612
$\mu$ (mm <sup>-1</sup> )	0.702	0.708
$\theta$ Range (°)	1.31–25.01	3.50–25.03
Unique reflections	8248	13518
Parameters	606	908
<i>R</i> <sub>int</sub>	0.0242	0.1128
Goodness of fit (GOF) on <i>F</i> <sup>2</sup>	1.049	0.922
<i>R</i> <sub>1</sub> <sup>a</sup>	0.0511	0.0601
<i>wR</i> <sub>2</sub> <sup>a</sup>	0.1330	0.1417
Maximum, minimum peaks (e Å <sup>-3</sup> )	0.839, -0.632	0.799, -0.373

$$^a I > 2\sigma(I), R_1 = \sum ||F_o| - |F_c|| / \sum |F_o|. wR_2 = \{ \sum [w(F_o^2 - F_c^2)^2] / \sum [w(F_o^2)^2] \}^{1/2}.$$

methane and methanol was stirred at room temperature for 2 h. The mixture color gradually changes from yellow to orange. The solvent was removed in a vacuum leaving an orange solid. Orange crystal of the complex suitable for an X-ray crystallograph structure determination was obtained by vapor diffusion of diethyl ether into solution of crude product in dichloromethane. Yield: 0.1725 g (55%). The crystalline solid was characterized by <sup>1</sup>H NMR and X-ray crystallography. <sup>1</sup>H NMR (400 MHz CDCl<sub>3</sub>)  $\delta$  (ppm): 1.71 (s, 4H, CH<sub>2</sub>), 2.48 (s, 6H, CH<sub>3</sub>), 2.94 (s, 6H, COCH<sub>3</sub>), 9.27 (s, 2H, NH), 8.22 (d, 2H, CH=CH), 7.74 (d, 2H, Napy), 8.35 (d, 2H, Napy), 8.54 (d, 2H, Napy), 6.86–6.99 (40H, Ph). ESI MS: *m/z* (%): 1409 [powders, M–BF<sub>4</sub>]<sup>+</sup>. Anal. Calc. For C<sub>74</sub>H<sub>74</sub>B<sub>2</sub>Cu<sub>2</sub>F<sub>8</sub>N<sub>6</sub>O<sub>6</sub>P<sub>4</sub> (crystals, 1568.01): C, 56.68; H, 4.76; N, 5.36. Found: C, 56.49; H, 4.68; N, 5.56%.

### 2.8. X-ray data collection and structure determinations

X-ray single-crystal diffraction data for complexes **1** and **2** were collected on a Bruker Smart and Nonius KappaCCD X-ray

diffractometer using a graphite monochromator with MoK $\alpha$  radiation ( $\lambda = 0.071073$  nm) at 293 K, respectively. The program SAINT was used for integration of the diffraction profiles. All structures were solved by direct method and refined by full-matrix least squares using SHELXL 97 program [40,41]. Metal atoms in each complex were located from the *E*-maps and other non-hydrogen atoms were located in successive different Fourier syntheses and refined with anisotropic thermal parameters on *F*<sup>2</sup>. The hydrogen atoms of the ligands were generated theoretically onto the specific atoms and refined isotropically with fixed thermal factors. Despite numerous attempts at growing better crystals and collecting better data, diffraction records of **2**·4H<sub>2</sub>O remain poor, which are indicated by the high *R*<sub>int</sub>. Hydrogen atoms of water in **2**·4H<sub>2</sub>O could not be localized, and remaining electronic density could not be assigned in a chemically meaningful way.

### 2.9. TD-DFT calculations

Time-dependent density functional theory (TD-DFT) calculations, employing B3LYP functional and 6-31G\* basis set, were carried out with the GAUSSIAN 03 program to predict and verify the absorption spectra of various species [42–44]. In order to simulate real experimental conditions, the default polarized continuum model (PCM/UA0) [42–44] in GAUSSIAN 03 program was also employed. So, all computational results presented here were carried out at TD-DFT(SCRF(PCM/UA0)-B3LYP/6-31G\*) level in CH<sub>2</sub>Cl<sub>2</sub> solution.

## 3. Results and discussion

### 3.1. Synthesis and characterization

The synthetic procedure to obtain ligand **L** is depicted in Scheme 2. 2,4-Dimethyl-7-acetylamino-1,8-naphthyridine was obtained by modification of a literature method [37] and its yield was improved by adjusting the pH 7–8. 7-Acetylamino-4-methyl-1,8-naphthyridine-2-aldehyde was synthesized using selenium dioxide in 1,4-dioxane as the oxidant. This was in contrast to the general procedure, which involves first converting the amine to an isoindole-1,3-dione group, brominating Ar–CH<sub>3</sub>, then hydrolyzing. The isolated yield (35%) was not very high, but the oxidation process was greatly simplified. **L**, [Cu(CH<sub>3</sub>CN)<sub>4</sub>](BF<sub>4</sub>) and PPh<sub>3</sub> or dppm were used as starting materials for the preparation of **1** and **2**. Two different kinds of coordination modes were observed for **L**, depending on the nature of the phosphine ligands. Reaction of a mixture of [Cu(CH<sub>3</sub>CN)<sub>4</sub>](BF<sub>4</sub>) and **L** with dppm gave CuNP<sub>2</sub><sup>+</sup> with a trigonal configuration, while copper(I) adopts a CuNOP<sub>2</sub><sup>+</sup> tetrahedral configuration in complex **1** with PPh<sub>3</sub>. Both complexes are air and moisture-stable at room temperature.

### 3.2. Crystal structures

Crystal structures of complexes **1** and **2** were obtained by X-ray diffraction. A summary of the crystallographic parameters and data

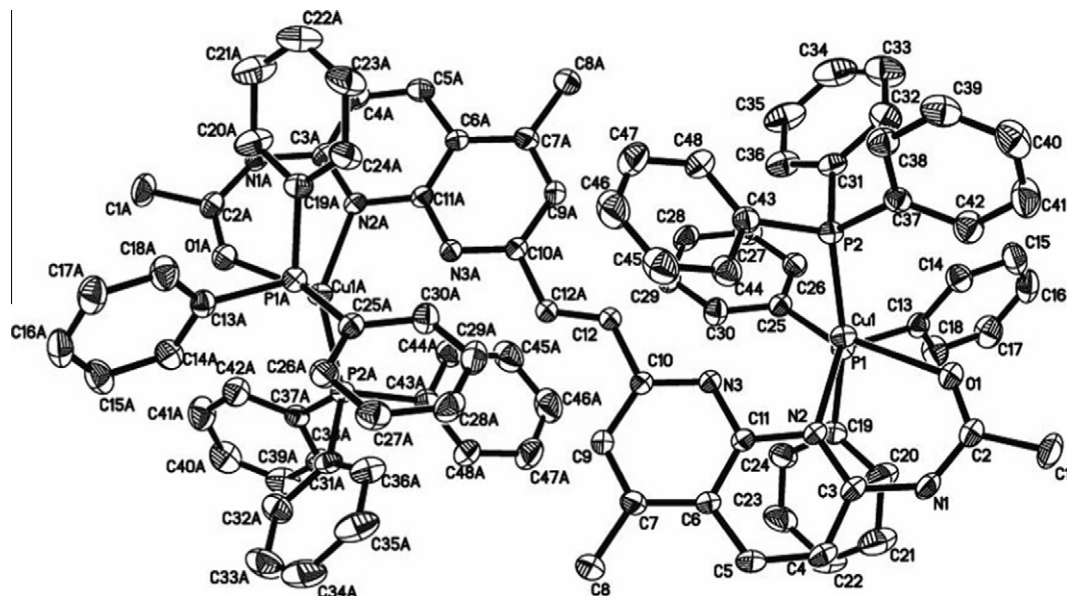


Fig. 1. Perspective drawing of  $\text{Cu}_2(\text{L})(\text{PPh}_3)_4(\text{BF}_4)_2$ , the thermal ellipsoids are drawn at 30% probability. The anions are omitted for clarity.

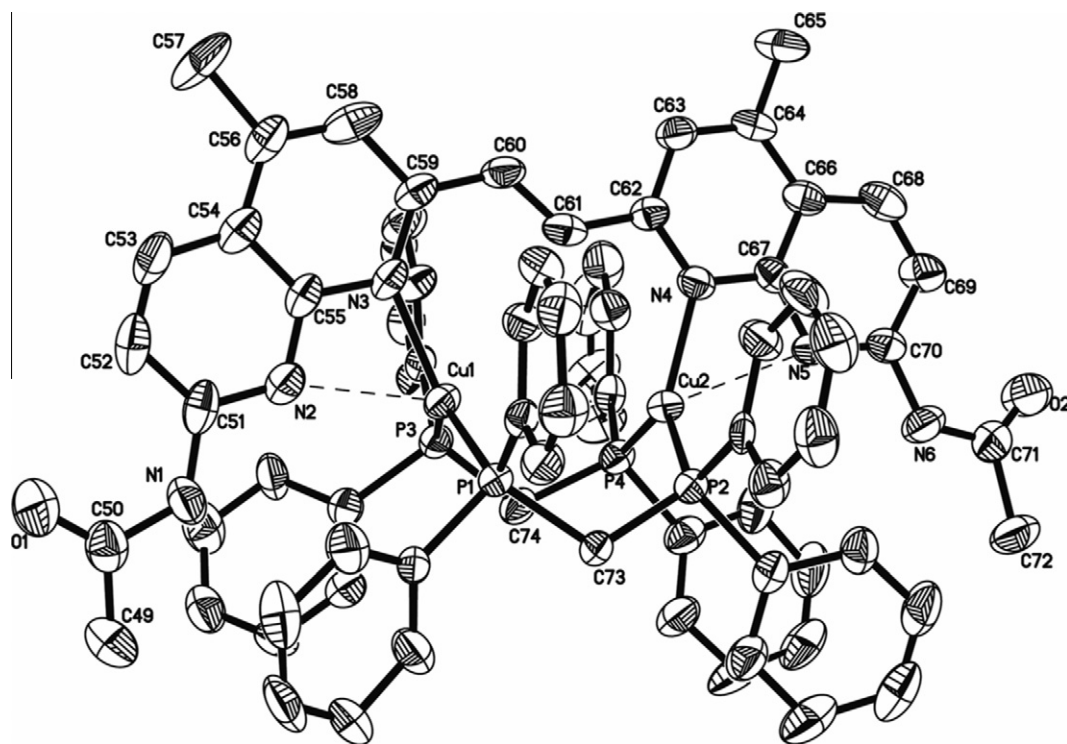


Fig. 2. Perspective drawing of  $\text{Cu}_2(\text{L})(\text{dppm})_2(\text{BF}_4)_2$ , the thermal ellipsoids are drawn at 30% probability. The anions are omitted for clarity.

is given in Table 1. Perspective drawings of their cations are depicted in Figs. 1 and 2 and selected bond lengths and angles are presented in Table 2. The coordination geometry of the Cu(I) atom in complex 1 is a distorted tetrahedron with each Cu(I) atom coordinated to the oxygen of a carbonyl group and a naphthyridyl nitrogen atom as well as two  $\text{PPh}_3$  ligands. A crystallographic inversion center is located at the vinylene group of **L**. The Cu(1)–P(2) and Cu(1)–P(1) distances are 2.242(1) and 2.285(1) Å, respectively. The different N(2)–Cu(1)–P(1) ( $106.93(9)^\circ$ ) and N(2)–Cu(1)–P(2) ( $125.22(9)^\circ$ ) angles are typical of related Cu(I) systems [33–35,45–47]. The Cu(1)–O(1) bond distance

(2.207(3) Å) falls in the range normally observed for analogous compounds, while the Cu(1)–N(2) distance of 2.102(3) Å is similar to those of typical four-coordinate copper(I) complexes [48,49]. The copper atom forms a six-membered ring with N(2)–Cu(1)–O(1) and C(2)–N(1)–C(3) angles of  $82.4(1)^\circ$  and  $130.8(4)^\circ$ , respectively. The six-membered ring and the adjacent naphthyridyl ring are not coplanar with a dihedral angle of  $2.6^\circ$ .

Compared with the structure of **1**, complex **2** containing bidentate ligand dppm exhibits two planar trigonal copper(I) centers and has a strained bimetallic 11-membered ring. Three-coordinate copper atoms are bonded to a nitrogen atom of ligand **L** and the

**Table 2**  
Selected bond lengths (Å) and bond angles (°) for **1** and **2**.

Complex 1					
Cu(1)–N(2)	2.102(3)	Cu(1)–O(1)	2.207(3)	Cu(1)–P(2)	2.243(1)
Cu(1)–P(1)	2.285(1)	P(1)–C(13)	1.823(4)	P(1)–C(25)	1.824(4)
P(1)–C(19)	1.834(4)	P(2)–C(37)	1.823(4)	P(2)–C(31)	1.828(4)
P(2)–C(43)	1.829(4)	O(1)–C(2)	1.209(5)	N(1)–C(3)	1.391(5)
N(2)–C(3)	1.318(5)	N(2)–C(11)	1.375(5)	N(3)–C(10)	1.324(5)
N(3)–C(11)	1.348(5)				
N(2)–Cu(1)–O(1)	82.4(1)	N(2)–Cu(1)–P(2)	125.2(1)	O(1)–Cu(1)–P(2)	109.2(1)
N(2)–Cu(1)–P(1)	106.9(1)	O(1)–Cu(1)–P(1)	97.6(1)	P(2)–Cu(1)–P(1)	123.18(4)
C(13)–P(1)–C(25)	103.7(2)	C(13)–P(1)–C(19)	102.0(2)	C(25)–P(1)–C(19)	104.8(2)
C(13)–P(1)–Cu(1)	115.4(1)	C(25)–P(1)–Cu(1)	117.5(1)	C(19)–P(1)–Cu(1)	111.8(1)
C(37)–P(2)–C(43)	101.9(2)	C(37)–P(2)–C(31)	101.8(2)	C(31)–P(2)–C(43)	104.8(2)
C(37)–P(2)–Cu(1)	120.0(1)	C(31)–P(2)–Cu(1)	111.6(1)	C(43)–P(2)–Cu(1)	114.8(1)
C(2)–O(1)–Cu(1)	130.1(3)	C(2)–N(1)–C(3)	130.8(4)	C(3)–N(2)–C(11)	117.5(3)
C(3)–N(2)–Cu(1)	131.8(3)	C(11)–N(2)–Cu(1)	110.5(2)	C(10)–N(3)–C(11)	117.5(3)
Complex 2					
Cu(1)–N(3)	2.083(6)	Cu(1)–P(3)	2.252(2)	Cu(1)–P(1)	2.259(2)
Cu(2)–N(4)	2.021(6)	Cu(2)–P(2)	2.223(2)	Cu(2)–P(4)	2.240(2)
N(1)–C(50)	1.38(1)	N(1)–C(51)	1.43(1)	O(1)–C(50)	1.22(1)
C(60)–C(61)	1.34(1)	N(3)–C(55)	1.355(9)	N(3)–C(59)	1.39(1)
P(1)–C(7)	1.815(7)	P(1)–C(1)	1.830(7)	P(1)–C(73)	1.848(6)
P(3)–C(31)	1.820(8)	P(3)–C(25)	1.836(8)	P(3)–C(74)	1.848(6)
N(3)–Cu(1)–P(3)	116.0(2)	N(3)–Cu(1)–P(1)	115.9(2)	P(3)–Cu(1)–P(1)	128.06(8)
C(61)–C(60)–C(59)	126.4(7)	N(3)–C(55)–N(2)	112.9(7)	N(2)–C(51)–N(1)	113.4(7)
C(50)–N(1)–C(51)	126.0(8)	O(1)–C(50)–N(1)	121.8(10)	O(1)–C(50)–C(49)	123.7(10)
C(7)–P(1)–C(1)	101.6(3)	C(7)–P(1)–C(73)	102.2(3)	C(1)–P(1)–C(73)	104.5(3)
C(7)–P(1)–Cu(1)	111.1(2)	C(1)–P(1)–Cu(1)	117.8(2)	C(73)–P(1)–Cu(1)	117.4(3)
C(31)–P(3)–C(25)	104.3(3)	C(31)–P(3)–C(74)	102.6(3)	C(25)–P(3)–C(74)	104.9(3)
C(31)–P(3)–Cu(1)	105.9(2)	C(25)–P(3)–Cu(1)	118.4(3)	C(74)–P(3)–Cu(1)	118.7(2)
C(55)–N(3)–C(59)	118.0(6)	C(55)–N(3)–Cu(1)	103.8(5)	C(59)–N(3)–Cu(1)	138.2(5)

**Table 3**  
Spectroscopic and photophysical properties of **1** and **2**.

Compound	Medium (298 K)	$\lambda_{\text{abs}}/\text{nm}$ ( $\epsilon/10^4 \text{ dm}^3 \text{ mol}^{-1} \text{ cm}^{-1}$ )	$\lambda_{\text{em}}/\text{nm}$ ( $\tau/\text{ns}$ )	$\phi_{\text{em}}$	$\lambda_{\text{abs}}/\text{nm}$ ( $\tau/\text{ns}$ ) <sup>a</sup>
<b>1</b>	CH <sub>3</sub> OH	375 (3.40), 382 (3.45)	408 (1.78) 423 (1.78)	0.401	
	CH <sub>3</sub> CN	370 (1.77), 380 (1.83) 415 (0.77)	405, 424	0.220	
	(CH <sub>3</sub> ) <sub>2</sub> CO	380 (2.85), 392 (2.75)	405, 424	0.066	450 (250, 12) 620 (150, 15)
	CH <sub>2</sub> Cl <sub>2</sub>	380 (2.34), 390 (2.52) 413 (1.39)	410, 430, 480 (4.21, 1.67)	0.002	
	solid		586 (6.5)		
<b>2</b>	CH <sub>3</sub> OH	374 (1.64), 383 (1.62) 413 (1.03)	410 (0.99), 428 (0.99)	0.278	500 (284), 550 (301) 620 (246), 650 (266)
	CH <sub>3</sub> CN	376 (2.21), 390 (1.96) 415 (0.45)	406, 425	0.161	
	(CH <sub>3</sub> ) <sub>2</sub> CO	370 (1.75), 391 (2.21) 416 (1.41)	404, 430	0.062	490 (266), 550 (380) 650 (348)
	CH <sub>2</sub> Cl <sub>2</sub>	373 (1.28), 396 (2.40) 418 (2.38)	410 (0.77), 437 (0.77) 470 (3.57, 1.67) 620 (1.71)	0.047	
	solid		620 (1.71)		
<b>L</b>	CH <sub>3</sub> OH	370, 388	409, 422		
	CH <sub>3</sub> CN	365	403		
	CH <sub>2</sub> Cl <sub>2</sub>	380, 400	410	0.39	
	solid		471, 482, 514, 540		

<sup>a</sup> Decay lifetime of transient difference absorption signals.

phosphorus atoms of two dppm ligands in a Y-shaped geometry with Cu(1)–P distances of 2.252(2) and 2.259(2) Å. The bond angles around the copper atom are 116.0(2)°, 115.9(2)° and 128.06(8)°. An interaction between the N(2) atom on the naphthyridyl ring and Cu(1) is observed with N(2)···Cu(1) distance of 2.501 Å, and the N(2)–Cu(1)–N(3), N(2)–Cu(1)–P(1) and N(2)–Cu(1)–P(3) bond angles are 58.32°, 99.57° and 105.24°, respectively. In contrast, N(5)···Cu(2) distance is 2.624 Å, and the N(4)–Cu(2)–N(5), N(5)–Cu(2)–P(4) and N(5)–Cu(2)–P(2) bond angles are 55.61°, 101.97° and 105.44°, respectively.

The average Cu–N(napy) distance of 2.052(6) Å in **2** is slightly shorter than that in **1** (2.102(3) Å), and the dihedral angle between the naphthyridyl planes is 10.4°. The dihedral angle between the two trigonal planes (Cu(1), N(3), P(3), P(1) and Cu(2), N(4), P(2), P(4)) is 36.9° and the Cu···Cu distance of 3.637 Å is significantly longer than the sum of the van der Waals radii of copper (2.8 Å) [50]. The Cu(2) atom adopts slightly distorted Y-shaped trigonal configuration with N(4)–Cu(2)–P(2), N(4)–Cu(2)–P(4) and P(2)–Cu(2)–P(4) bond angles of 120.8(2)°, 114.9(2)° and 124.19(8)°, respectively. The bond lengths of Cu(2)–N(4) (2.021(6) Å),

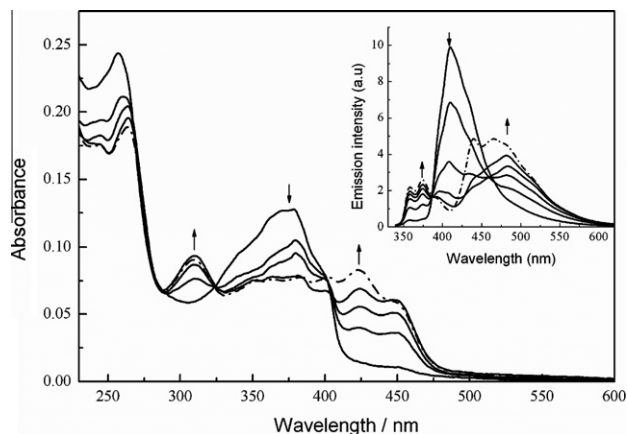


**Fig. 3.** Absorption spectra changes during 365 nm light irradiation of **L** over a period of 4 min in dichloromethane at 298 K. Inset: emissive spectral changes accompanying the photochromism of **L** in dichloromethane with excitation at 320 nm.

Cu(2)–P(2) (2.223(2) Å) and Cu(2)–P(4) (2.240(2) Å) are significantly shorter than those around the Cu(1) atom.

### 3.3. Electronic absorption spectra

The spectral data of UV–Vis absorption for **L**, **1** and **2** in different solvents are summarized in Table 3. The absorption spectrum of **L** exhibits a broad band (350–400 nm) which can be assigned to a spin-allowed  $\pi \rightarrow \pi^*$  transition (Fig. 3). The absorptions of **L**, **1** and **2** are sensitive to the solvent and exhibit a blue shift as the solvent polarity increases (see the Supporting information Fig. S1). Low energy absorption bands appear in the region of 400, 413 and 418 nm for **L**, **1** and **2** in dichloromethane, respectively. A TD-DFT calculation of **1** and **2** demonstrated that their highest occupied molecular orbital (HOMO) and lowest unoccupied molecular orbital (LUMO) are mainly localized on the phosphine ligand

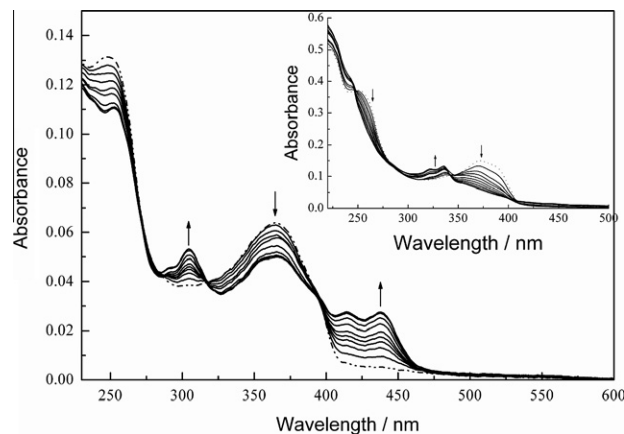


**Fig. 5.** Changes of absorption spectra during 365 nm light irradiation of **L** in acetonitrile or methanol (inset) at 298 K.

and the naphthyridine moiety, respectively. The calculated energy gaps of  $\Delta E_{406 \rightarrow 417}$  and  $\Delta E_{416 \rightarrow 417}$  for **1** are 3.3599 eV (369 nm) and 2.5631 eV (484 nm) and corresponding oscillator strength ( $f$ ) values are 0.8427 and 0.0124, respectively (Fig. S2), whereas those of  $\Delta E_{337 \rightarrow 343}$  and  $\Delta E_{342 \rightarrow 343}$  for **2** are 2.9888 eV (415 nm) and 2.2880 eV (542 nm), and with oscillator strength ( $f$ ) values of 0.8905 and 0.0253, respectively (Fig. 4). Thus the observed lower-energy absorption bands with large extinction coefficients ( $10^4 \text{ M}^{-1} \text{ cm}^{-1}$ ) for **1** and **2** are assigned to ligand-to-ligand charge transfer (LLCT, phosphine  $\rightarrow$  napy) transition in nature.

### 3.4. Photoinduced structural conversion

Upon irradiation of a degassed dichloromethane solution of **L** at 365 nm, a photoinduced structural conversion takes place, which is accompanied by a change of the solution from colorless to yellowish-green. The changes in the UV–Vis absorption and emission spectra recorded during irradiation at 365 nm over a period of

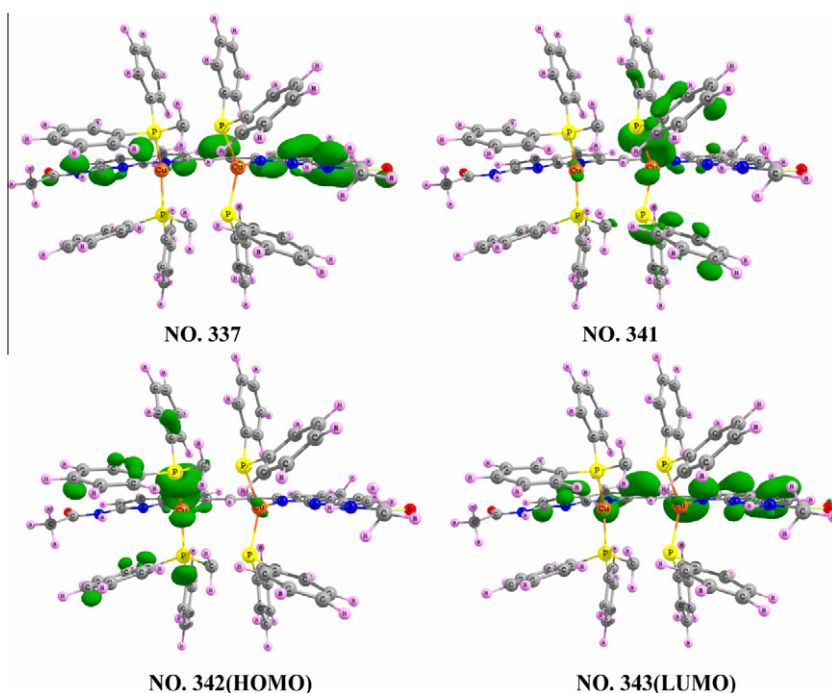


**Fig. 4.** Plots of the relevant HOMO and LUMO for complex **2**.

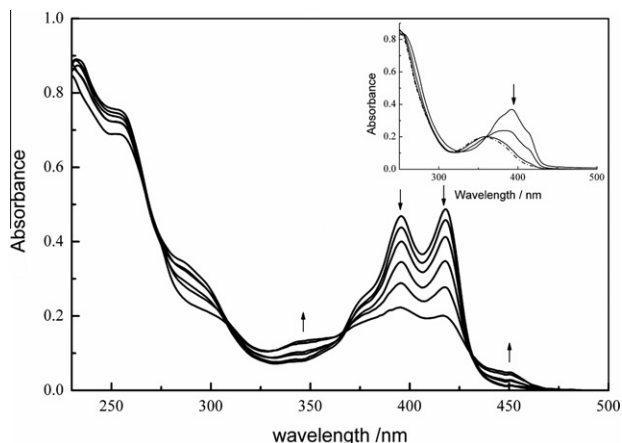


**Fig. 6.** Absorption spectra changes during 365 nm light irradiation of **1** (inset) and **2** in dichloromethane at 298 K.

4 min at room temperature are displayed in Fig. 3. The process is characterized by isosbestic points in the absorption spectra at 324 and 404 nm. The absorption feature at 365 nm decreased with a concomitant increase in the absorption at 310, 423 and 450 nm. Deviation in the isosbestic point at 404 nm is observed over longer irradiation times indicating subsequent photoisomerization of **L**. During the period with irradiation at 365 nm, the band at 410 nm in the emission spectra of **L** rapidly weakened while four new emission peaks appeared at 358, 375, 439 and 481 nm upon excitation at 320 nm. Though the color changes in dichloromethane were largely reversible, the initial absorption profile was not completely restored even after the solution was kept in the dark for 4 days at room temperature (Fig. S3).

A comparison of the spectral data for **L** in different solvents indicates that the evolution of the photochromic process can be tuned by varying the polarity of the solvent (Figs. 3 and 5). For **L** in acetonitrile and dichloromethane solutions, upon irradiation at 365 nm, the changes observed in the low-energy absorption band are tentatively attributed to a proton transfer from the amidocyanogen group to an adjacent naphthyridine-N atom resulting in an intramolecular hydrogen bond with the oxygen atom of the carbonyl moiety [51,52]. Similar 1,3-hydrogen transfer has been reported on 1,8-naphthyridyl derivatives and their crystal structures were characterized [53]. Moreover, absorption spectra of **L** in protic solvent methanol demonstrate that solvent polarity has profound influence on the hydrogen atom transfer, and the low-energy absorption band was not observed due to the interaction between solvent protons and the naphthyridine-N atoms (Fig. 5). Changes of the high-energy absorption band around

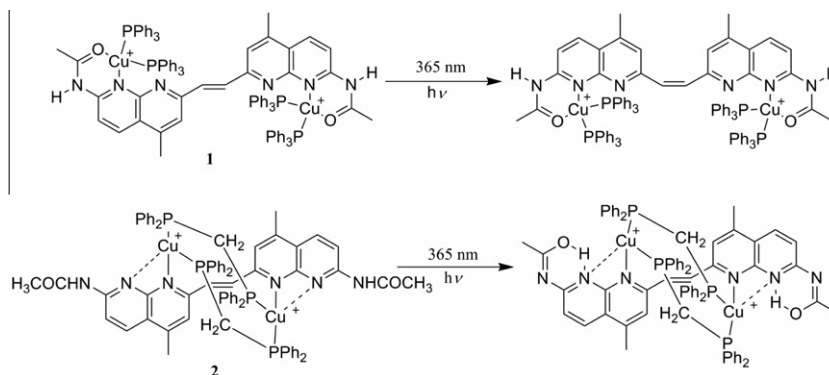
315 nm in protic and aprotic solvents imply that a photoinduced isomerization reaction also occurs from the *trans*- to *cis*-conformations.

Fig. 6 illustrates a typical sequence of spectra observed following irradiation of **1** and **2** at 365 nm in dichloromethane solution. The absorption spectra of **1** display a clear progression of the isomerization from *trans* to *cis*-conformations, and the peak in the initial spectrum with  $\lambda_{\max}$  at 393 nm exhibits a blue shift to 360 nm during irradiation. Irradiation of **2** in dichloromethane affords absorption spectra with isosbestic points at 310, 367 and 430 nm as well as two new bands at 345 and 450 nm, and the absorption bands at 373, 396 and 418 nm weaken. Overall, the spectral changes for **2** are very different from those of **1** but low-energy absorption bands are similar to those found for ligand **L** in dichloromethane solution, indicating that considerable amounts of the imino-tautomer (Scheme 3) [54,55]. The spectral observations of **1** and **2** also provide strong evidence for the mechanistic interpretation of the photoinduced isomerization reaction and an intramolecular proton transfer of ligand **L** in organic solvents.

Generally, the steric hindrance inherent in a ligand or induced by formation of a metal complex will increase the molecular rigidity thereby preventing the intramolecular conformational conversion. In contrast to ligand **L**, the markedly slow changes in the low energy absorption bands of **1** upon irradiation at 365 nm indicate that proton transfer is less facile because of the existence of bonding interactions between the copper(I) center and nitrogen and oxygen atoms. While the changes in the absorption spectra of **2** are probably caused by the free acetyl amino group allowing 1,3-hydrogen transfer to occur readily during irradiation.

### 3.5. Emission spectra

Upon excitation at 380 nm, **L** exhibits well-structured emission at 473, 512 and 545 nm in the solid state at room temperature, and vibration progressions ranging from 1180 to 1610  $\text{cm}^{-1}$  are close to C=C and C=N stretching frequencies of **L** (Fig. 7). Emissive spectral changes were recorded during 365 nm irradiation of **L** in acetonitrile and methanol with excitation at 310 nm. Figs. 5 and 8 illustrate the emissive spectral changes accompanying the photochromism of **L** in both acetonitrile and methanol. In acetonitrile solution a new emission peak following irradiation (365 nm) appeared at 490 nm, while in the case of methanol solution a characterized emission peak at 410 nm for **L** weakened and blue-shifted to 390 nm. This is in good agreement with the photoinduced structural conversion in different solvents mentioned above. Complexes **1** and **2** display intense room-temperature solid-state emissions with  $\lambda_{\max}$  at 586 and 620 nm, respectively. The energy and the shape of the emission bands are clearly different from that of the ligand, and can be tentatively attributed to a mixture of MLCT



**Scheme 3.** Photoinduced intramolecular structural conversion of **1** and **2**.

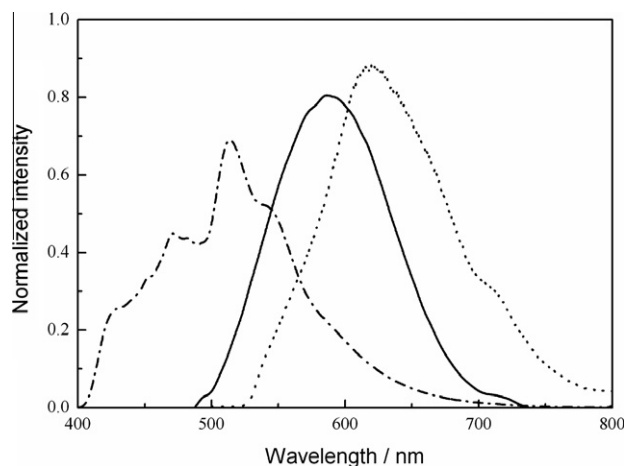


Fig. 7. Room-temperature solid-state emission spectra of **L** (dashed dot line), **1** (solid line) and **2** (dot line) excitation at 380 nm at 298 K.

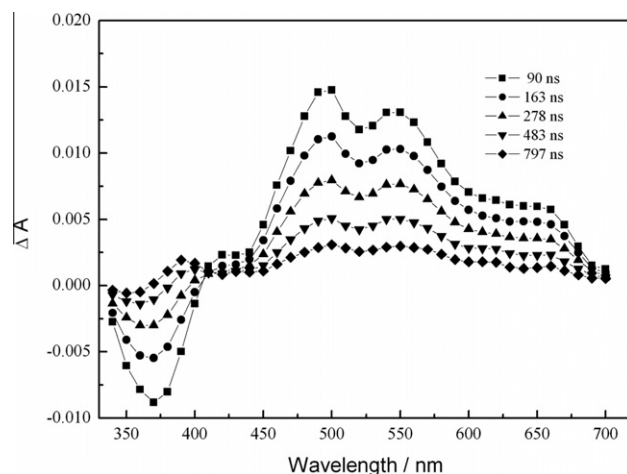


Fig. 9. Room temperature time-resolved difference absorption spectra of **2** ( $3.2 \times 10^{-5}$  M) recorded at 100 ns after excitation at 355 nm in degassed acetone solution.

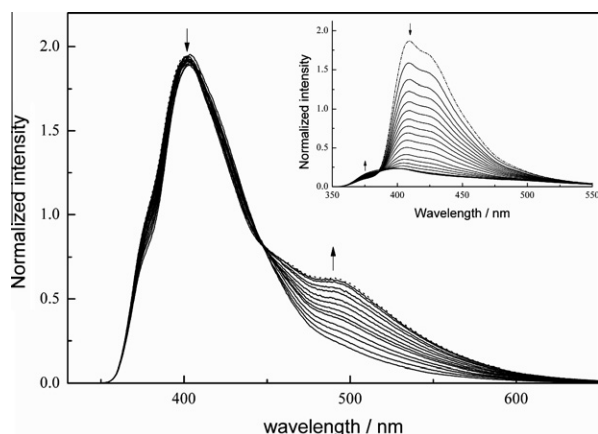


Fig. 8. Emissive spectral changes accompanying the photochromism of **L** in acetonitrile and methanol (inset) with excitation at 310 nm at 298 K.

and LLCT origin. However, short emission lifetimes of  $\tau < 10$  ns do not reflect the character of a typical  $^3\text{MLCT}$  excited state. In organic solvents such as methanol, acetonitrile, dichloromethane and acetone, **L**, **1** and **2** show strong emission ranging from 400 to 440 nm (Fig. 3 and Fig. S4, Table 3). Shorter emission lifetimes of 1–2 ns and the large overlap between emission and the lowest-energy absorption band suggest that the emissions originate from intraligand excited state in nature. However, upon excitation at 420 nm, **1** and **2** display weak, low-energy emission maxima at 480 and 470 nm with the emission lifetimes of  $< 4$  ns in degassed dichloromethane solution, respectively (Fig. S5). Observed dual fluorescent phenomena indicate that two emissive species with considerable amounts present in the solution. Attempts to obtain the compounds were unsuccessful.

### 3.6. Time-resolved absorption spectra

Time-resolved absorption spectra of **1** and **2** in methanol or acetone solution were measured at room temperature following nano-second-pulsed excitation at 355 nm. The transient absorption spectra of **2** show intense absorption with  $\lambda_{\text{max}}$  at 490–550 nm and a tail beyond 650 nm in acetone solution (Fig. 9); in methanol the absorption spectra display a blue shift to 450 nm (Fig. 10). Complex **1** exhibits a weak transient absorption spectrum, with a broad absorption band appearing from 350 to 700 nm (Fig. S6). A

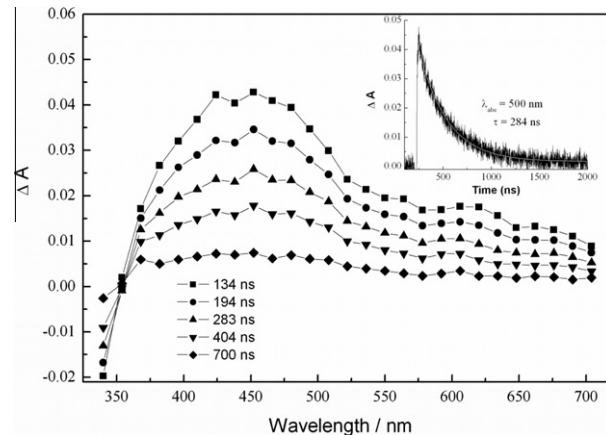


Fig. 10. Room temperature time-resolved difference absorption spectra of **2** ( $3.0 \times 10^{-5}$  M) recorded at 100 ns after excitation at 355 nm in degassed methanol solution. Inset: decay traces of transient difference absorption spectra of **2** monitored at 500 nm.

comparison of the lifetimes of the transient absorption signals for **1** and **2** with the corresponding emission lifetimes in methanol or acetone implies that the transient absorptions probably originate from a new species generated upon laser flash photolysis (Fig. S7) [56,57].

## 4. Conclusions

The new ligand 1,2-bis[2-(4-methyl-7-acetylamino-1,8-naphthyridine)]ethylene and two kinds of luminescent binuclear copper(I) complexes containing **L** and  $\text{PPh}_3$  or  $\text{dppm}$  were prepared. X-ray crystal analysis revealed that the different coordination geometries of the copper(I) centers,  $\text{O}(\text{N})\text{CuP}_2^+$  and  $\text{NCuP}_2^+$ , depend on the nature of the phosphine ligands. Upon irradiation at 365 nm, a photoinduced isomerization reaction from the *trans*- to *cis*-conformations of **L** and complex **1** and intramolecular proton transfer involving the free acetylamino group of **L** and complex **2** were observed through the combination of absorption and emission spectra in different solvents at room temperature. The parallel processes depend on the solvent polarity and nature of phosphine ligand. Spectroscopic investigations suggest that the intense solid-state emissions of **L** and the complexes originate from  $\pi\pi^*$  and

MLCT/LLCT transitions, respectively, whereas transient absorption of the complexes results from a new species.

### Acknowledgments

The work was supported by the National Natural Science Foundation of China (NSFC Grant No. 21071123) and the foundation (GJHZ200817) for Bureau of International Co-operation of Chinese Academy of Science. We thank Program for Changjiang Scholars and Innovative Research Team in University (IRT0979) for the financial support.

### Appendix A. Supplementary material

CCDC 764387 and 268336 contain the supplementary crystallographic data for this paper. These data can be obtained free of charge from The Cambridge Crystallographic Data Centre via [www.ccdc.cam.ac.uk/data\\_request/cif](http://www.ccdc.cam.ac.uk/data_request/cif). UV–Vis absorption and emission spectra of **1** and **2** in degassed CH<sub>2</sub>Cl<sub>2</sub>, (CH<sub>3</sub>)<sub>2</sub>CO, CH<sub>3</sub>CN, CH<sub>3</sub>OH at 298 K; UV–Vis absorption and emissive spectral changes during 365 nm light irradiation of **L** in CH<sub>3</sub>CN, CH<sub>3</sub>OH at 298 K. Room temperature time-resolved difference absorption spectra of **1** in degassed (CH<sub>3</sub>)<sub>2</sub>CO solution; decay traces of transient difference absorption spectra of **2** monitored at 490 nm after excitation at 355 nm in degassed (CH<sub>3</sub>)<sub>2</sub>CO solution. Supplementary data associated with this article can be found, in the online version, at doi:10.1016/j.ica.2011.09.014.

### References

- [1] E.A. Smith, M. Kyo, H. Kumasawa, K. Nakatani, I. Saito, R.M. Corn, *J. Am. Chem. Soc.* 124 (2002) 6810.
- [2] T. Peng, K. Nakatani, *Angew. Chem., Int. Ed.* 44 (2005) 7280.
- [3] T.F.A. de Greef, G.B.W.L. Ligthart, M. Lutz, A.L. Spek, E.W. Meijer, R.P. Sijbesma, C. Dohno, S.N. Uno, K. Nakatani, *J. Am. Chem. Soc.* 130 (2008) 5479.
- [4] N. Minakawa, S. Ogata, M. Takahashi, A. Matsuda, *J. Am. Chem. Soc.* 131 (2009) 1644.
- [5] A. Kobori, K. Nakatani, *Bioorg. Med. Chem.* 16 (2008) 10338.
- [6] C. Dohno, S.N. Uno, S. Sakai, M. Oku, K. Nakatani, *Bioorg. Med. Chem.* 17 (2009) 2536.
- [7] (a) C. Dohno, S.N. Uno, K. Nakatani, *J. Am. Chem. Soc.* 129 (2007) 11898; (b) F. Takei, H. Suda, M. Hagihara, J. Zhang, A. Kobori, K. Nakatani, *Chem. Eur. J.* 13 (2007) 4452.
- [8] W.W. Paudler, T.J. Kress, *Adv. Heterocycl. Chem.* 11 (1970) 123.
- [9] W.W. Paudler, R.M. Sheets, *Adv. Heterocycl. Chem.* 33 (1983) 147.
- [10] A. Sinha, S.M. Wahidur Rahaman, M. Sarkar, B. Saha, P. Daw, J.K. Bera, *Inorg. Chem.* 48 (2009) 11114.
- [11] K.P. Dixon, *Inorg. Chem.* 16 (1977) 2618.
- [12] M. Maekawa, M. Munakata, S. Kitagawa, T. Kuroda-Sowa, Y. Suenaga, M. Yamamoto, *Inorg. Chim. Acta* 271 (1998) 129.
- [13] C. Bianchini, H.M. Lee, P. Barbaro, A. Meli, S. Moneti, F. Vizza, *New J. Chem.* 23 (1999) 929.
- [14] J.M. Epstein, J.C. Dewan, D.L. Kepert, A.H. White, *J. Chem. Soc., Dalton Trans.* (1974) 1949.
- [15] J.C. Dewan, D.L. Kepert, A.H. White, *J. Chem. Soc., Dalton Trans.* (1975) 490.
- [16] D. Gatteschi, C. Mealli, L. Sacconi, *Inorg. Chem.* 15 (1976) 2774.
- [17] D.G. Hendricker, R.J. Foster, *Inorg. Chem.* 12 (1973) 349.
- [18] R.J. Staniewicz, R.F. Sympson, D.G. Hendricker, *Inorg. Chem.* 16 (1977) 2166.
- [19] R.J. Staniewicz, D.G. Hendricker, *J. Am. Chem. Soc.* 99 (1977) 6581.
- [20] J.-L. Zuo, W.-F. Fu, C.-M. Che, K.K. Cheung, *Eur. J. Inorg. Chem.* (2003) 255.
- [21] R. Zong, R.P. Thummel, *J. Am. Chem. Soc.* 127 (2005) 12802.
- [22] J.K. Bera, N. Sadhukhan, M. Majumdar, *Eur. J. Inorg. Chem.* 48 (2009) 4023.
- [23] H. Nakajima, K. Tanaka, *Angew. Chem., Int. Ed.* 38 (1999) 362.
- [24] C. He, S.J. Lippard, *J. Am. Chem. Soc.* 122 (2000) 184.
- [25] C.H. Chien, J.C. Chang, C.Y. Yeh, G.H. Lee, J.M. Fang, S.M. Peng, *Dalton Trans.* (2006) 2106.
- [26] S.L. Schiavo, M. Grassi, G.D. Munno, F. Nicolo, D.G. Tresoldi, *Inorg. Chim. Acta* 216 (1994) 209.
- [27] H. Nakajima, H. Nagao, K. Tanaka, *J. Chem. Soc., Dalton Trans.* (1996) 1405.
- [28] C. He, J.L. DuBois, B. Hedman, K.O. Hodgson, S.J. Lippard, *Angew. Chem., Int. Ed.* 40 (2001) 1484.
- [29] C.-M. Che, C.-W. Wan, K.-Y. Ho, Z.-Y. Zhou, *New J. Chem.* 25 (2001) 63.
- [30] Y. Chen, W.-F. Fu, J.-L. Li, X.-J. Zhao, X.-M. Ou, *New J. Chem.* 31 (2007) 1785.
- [31] Y. Chen, X.-J. Zhao, X. Gan, W.-F. Fu, *Inorg. Chim. Acta* 361 (2008) 2335.
- [32] W.-F. Fu, H.-F.-J. Li, D.-H. Wang, L.-J. Zhou, L. Li, X. Gan, Q.-Q. Xu, H.-B. Song, *Chem. Commun.* (2009) 5524.
- [33] J.-F. Zhang, W.-F. Fu, X. Gan, J.-H. Chen, *Dalton Trans.* (2008) 30930.
- [34] H.-M. Zhang, W.-F. Fu, J. Wang, X. Gan, Q.-Q. Xu, S.-M. Chi, *Dalton Trans.* (2008) 6817.
- [35] Y. Chen, J.-S. Chen, X. Gan, W.-F. Fu, *Inorg. Chim. Acta* 362 (2009) 2492.
- [36] H. Araki, K. Tsuge, Y. Sasaki, S. Ishizaki, N. Kitamura, *Inorg. Chem.* 46 (2007) 10032.
- [37] R.A. Henry, P.R. Hammond, *J. Heterocycl. Chem.* 14 (1977) 1109.
- [38] F. Liang, Z.-Y. Xie, L.-X. Wang, X.-B. Jing, F.-S. Wang, *Tetrahedron Lett.* 43 (2002) 3427.
- [39] M.A. Fakhfakh, A. Fournet, E. Prina, J.F. Mouscadet, X. Franck, R. Hocquemiller, B. Figadéra, *Bioorg. Med. Chem.* 11 (2003) 5013.
- [40] G.M. Sheldrick, *SHELXS 97*, Program for the Solution of Crystal Structure, University of Göttingen, 1997.
- [41] G.M. Sheldrick, *SHELXL97*, Program for the Refinement of Crystal Structures, University of Göttingen, Germany, 1997.
- [42] A.D. Becke, *J. Chem. Phys.* 98 (1993) 5648.
- [43] C. Lee, W. Yang, R.G. Parr, *Phys. Rev. B* 37 (1988) 785.
- [44] M.J. Frisch, G.W. Trucks, H.B. Schlegel, G.E. Scuseria, M.A. Robb, J.R. Cheeseman, J.A. Montgomery, T. Vreven Jr., K.N. Kudin, J.C. Burant, J.M. Millam, S.S. Iyengar, J. Tomasi, V. Barone, B. Mennucci, M. Cossi, G. Scalmani, N. Rega, G.A. Petersson, H. Nakatsuji, M. Hada, M. Ehara, K. Toyota, R. Fukuda, J. Hasegawa, M. Ishida, T. Nakajima, Y. Honda, O. Kitao, H. Nakai, M. Klene, X. Li, J.E. Knox, H.P. Hratchian, J.B. Cross, C. Adamo, J. Jaramillo, R. Gomperts, R.E. Stratmann, O. Yazyev, A.J. Austin, R. Cammi, C. Pomelli, J.W. Ochterski, P.Y. Ayala, K. Morokuma, G.A. Voth, P. Salvador, J.J. Dannenberg, V.G. Zakrzewski, S. Dapprich, A.D. Daniels, M.C. Strain, O. Farkas, D.K. Malick, A.D. Rabuck, K. Raghavachari, J.B. Foresman, J.V. Ortiz, Q. Cui, A.G. Baboul, S. Clifford, J. Cioslowski, B.B. Stefanov, G. Liu, A. Liashenko, P. Piskorz, I. Komaromi, R.L. Martin, D.J. Fox, T. Keith, M.A. Al-Laham, C.Y. Peng, A. Nanayakkara, M. Challacombe, P.M.W. Gill, B. Johnson, W. Chen, M.W. Wong, C. Gonzalez, J.A. Pople, *GAUSSIAN 03*, Revision C.02, GAUSSIAN, Inc., Wallingford, CT, 2004.
- [45] W.-F. Fu, X. Gan, J. Jiao, Y. Chen, M. Yuan, S.-M. Chi, M.-M. Yu, S.-X. Xiong, *Inorg. Chim. Acta* 360 (2007) 2758.
- [46] Q.-Q. Xu, D.-H. Wang, S.-M. Chi, X. Gan, W.-F. Fu, *Inorg. Chim. Acta* 362 (2009) 2529.
- [47] P.J. Burke, D.R. McMillin, W.R. Robinson, *Inorg. Chem.* 19 (1980) 1211.
- [48] C. He, S.J. Lippard, *Inorg. Chem.* 39 (2000) 5225.
- [49] X.-M. Zhang, M.-L. Tong, X.-M. Chen, *Angew. Chem., Int. Ed.* 141 (2002) 1029.
- [50] A. Bondi, *J. Phys. Chem.* 68 (1964) 441.
- [51] J. Abou-Zied, R. Jimenez, E.H.Z. Thompson, D.P. Millar, F.E. Romesberg, *J. Phys. Chem. A* 106 (2002) 3665.
- [52] J. Seo, S. Kim, S.Y. Park, *J. Am. Chem. Soc.* 126 (2004) 11154.
- [53] W.-F. Fu, L.-F. Jia, W.-H. Mu, X. Gan, J.-B. Zhang, P.-H. Liu, Q.-Y. Cao, G.-J. Zhang, L. Quan, X.-J. Lv, Q.-Q. Xu, *Inorg. Chem.* 49 (2010) 4524.
- [54] J. Fahrni, M.M. Henary, D.G. VanDerveer, *J. Phys. Chem. A* 106 (2002) 7655.
- [55] W.S. Yu, C.C. Cheng, Y.M. Cheng, P.C. Wu, Y.H. Song, Y. Chi, P.T. Chou, *J. Am. Chem. Soc.* 125 (2003) 10800.
- [56] P. Lainé, F. Bedioui, E. Amouyal, V. Albin, F. Berruyer-Penaud, *Chem. Eur. J.* 8 (2002) 3162.
- [57] S. Chakraborty, T.J. Wadas, H. Hester, R. Schmehl, R. Eisenberg, *Inorg. Chem.* 44 (2005) 6865.